

Silicon photonic subwavelength grating based integrated optical delay lines

Reza Ashrafi¹, Junjia Wang¹, Ivan Glesk², and Lawrence R. Chen¹

¹Department of Electrical and Computer Engineering, McGill University, Montreal, QC H3A 0E9 Canada

²Department of Electronic and Electrical Engineering, University of Strathclyde, Glasgow, G1 1XU, UK

Abstract: We demonstrate a novel integrated optical delay line approach based on silicon subwavelength gratings (SWGs). By 30% change in duty-cycle of SWG waveguides with a same length of 8mm to control their group index, up to ~30ps time-delay was achieved.

1. Introduction

Optical delay line (ODL) devices are fundamental building blocks in all-optical and microwave photonic signal processing circuits. Some of the all-optical processing devices, e.g. optical Hilbert transformers and differentiators, employ the ODLs for synthesizing their finite impulse response (FIR) [1]. In microwave photonic signal processing, ODLs constitute basic building block for implementation of beam forming networks for phased array antennas [2], ultra-wideband pulse shapers [3], and microwave photonic filters (MPFs) [4]. Among different ODL approaches such as those based on all-fiber and micro-electro-mechanical-system (MEMS) technologies [5-7], integrated waveguide ODL solutions [8,9] provide more temporal resolutions and are more compact than other implementations.

In both types of fixed [8] or reconfigurable [9] ODL structures in previous implementations, the time-delay difference between the taps of the ODL have been achieved through changing the waveguide length in each stage of the structure. This has led to a geometrical complex waveguide structure to achieve the required incremental time steps between the taps of the ODL device [8,9].

In this work, we present a novel ODL solution based on subwavelength grating (SWG) waveguides. This approach reduces considerably the complexity of the waveguide structure by providing the required incremental time-delay difference between the taps of the ODL, through a precise change of the effective (and group) index in each waveguide branch.

2. Device design and layout

Fig. 1 shows a schematic of our proof-of-principle demonstration, which is a 4-tap ODL device on silicon-on-insulator (SOI) platform. In each tap one SWG waveguide, all with the same length of L , has been fabricated. SWGs are new types of micro-photonic waveguides which offer high flexibility in terms of tailoring the effective index and dispersion [10]. An SWG waveguide is a grating structure

with a period that is smaller than the wavelength of light. In our SOI implementation, the SWG waveguides have realized by alternating periodically segments of silicon and silica, with a period of Λ along the propagation direction. The propagating mode in SWGs is referred to as Bloch mode [10]. By choosing the duty cycle defined as $D = a / \Lambda$, the effective index of the SWG waveguide can be modified and hence, the propagation properties of the Bloch mode can be controlled, where a is the width of the silicon segment in each period, see Fig. 1. The effective refractive index of the propagating Bloch mode in each tap of the fabricated ODL is a function of D , i.e. $n_e(i) = f(D_i)$. See Ref. [11,12] for a detailed numerical analysis about this. The corresponding generated time-delay difference between the taps of the ODL device can be expressed as

$$\Delta t(i) = [n_e(i+1) - n_e(i)] \cdot L / c, \quad 1 < i < N-1 \quad (1)$$

where c is the light speed in vacuum, and $N=4$ is the number of taps in the ODL. By properly designing the duty cycle D_i in each waveguide, the temporal separation between the taps can be controlled.

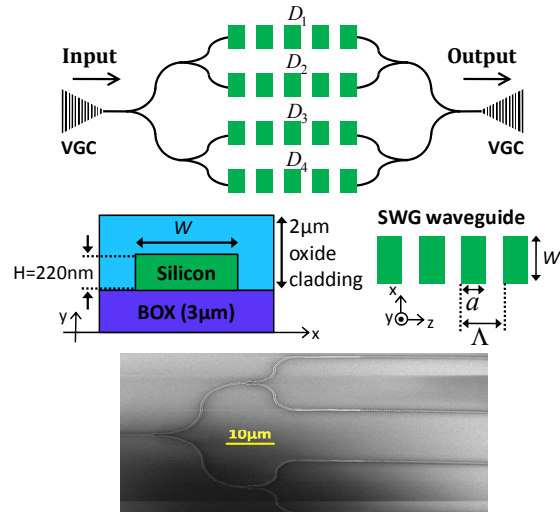


Fig. 1. Schematic and an SEM image of our fabricated 4-tap ODL structure based on SWG waveguides in SOI. The waveguide cross-section and parameters for the SWG waveguides are also illustrated.

A schematic of an SWG waveguide is shown in Fig. 1: the silicon SWG waveguide (with cross-sectional dimensions $W \times H$) sits on top of a buried oxide (BOX) layer and is covered by an index-matched silica cladding layer. Two SWG tapers in each SWG waveguide (not illustrated in Fig. 1), are used to convert light into (and from) a Bloch mode before (and after) propagating through the SWG waveguide [10].

The ODL device were fabricated using electron beam lithography and a full etch. The Si waveguides have a thickness of 220 nm on top of a 3 μm BOX layer on a Si substrate. The waveguide width W is 500 nm, the SWG grating period is 300 nm, and the SWG waveguide length is $L = 8\text{mm}$. The SWG taper has a period of 200 nm, and the width varies from $W_1 = 500$ nm down to $W_2 = 200$ nm over a length of 15 μm . The designed duty cycles in SWG waveguides are $D_1=60\%$, $D_2=50\%$, $D_3=40\%$, and $D_4=30\%$. Six Y-branches (with 50:50 splitting ratio) were used to split and collect the optical power at the input and output of the SWG waveguides, respectively. Vertical grating couplers (VGCs) are used to couple light into and out of the ODL device and are optimized for TE transmission.

3. Experimental results

Fig. 2 shows the measured spectral response of the fabricated ODL device. At the input, we launch a Gaussian-like optical pulse with a full width at half maximum (FWHM) bandwidth of 2 nm at a central wavelength of 1556 nm, which is generated using an actively mode-locked fiber laser (MLL, Pritel Inc.) with a repetition rate of 10 GHz. Fig. 3 shows the generated time-domain output pulse train, measured using optical sampling oscilloscope. The signal spectrum at the input and output of the ODL device is also shown in the inset of Fig. 3. As it can be seen in Fig. 3, the generated time-delay difference between the taps of the ODL by introducing 10% change in duty cycles of SWG waveguides with 8 mm length is $\sim 9\text{ps}$. According to Eq. (1), this time-delay difference between the taps corresponds to an effective refractive index difference of 0.338 between the SWG waveguides. Note that as shown in Fig. 3, the pulse propagating through the SWG waveguide with lowest duty cycle (i.e. D_4) arrives faster than the other branches.

An important practical consideration concerns the fact that as studied in [12], the interaction between the field and the vertical edges of the silicon blocks causes unwanted scattering loss due to wall roughness. As we have observed in the temporal response of our device, this loss is increased normally by decreasing the duty cycle of

the SWG waveguides. This can be seen in Fig. 3, where the output pulse corresponding to the waveguide branch with $D_4=30\%$ has the most amount of propagation loss. This additional loss can be compensated by properly designing the Y-branches with non 50:50 splitting ratios.

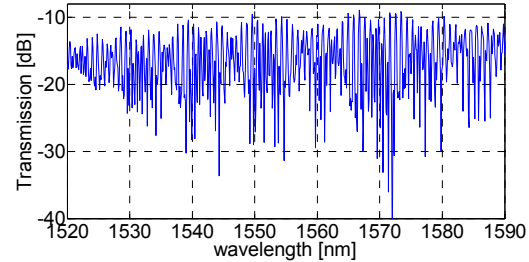


Fig. 2. Measured spectral response of the fabricated ODL.

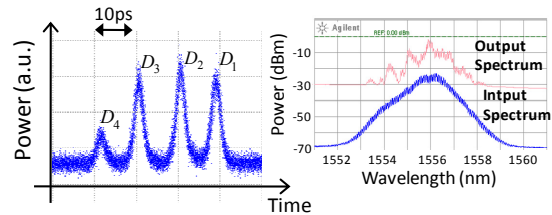


Fig. 3. Generated pulse train at the output of the fabricated ODL device in response to a single input optical pulse. Input and output signal spectra have also shown in the inset.

4. Conclusions

We have demonstrated a novel ODL approach based on SWG waveguides in SOI. The obtained results clearly prove a great capability of the SWG waveguides to be employed in ODLs to achieve a considerably compact structure. The reported experimental demonstration of the integrated silicon photonic ODL device in this work is a fundamental step towards the development of many integrated all-optical and microwave photonics signal generation and processing circuits.

References

1. N. Q. Ngo and Y. Song, *Opt. Lett.*, **36**(6), pp. 915-917, 2011.
2. R. J. Mailloux, *Phased Array Antenna Handbook* (Artech House, Boston, MA, 2005).
3. R. Adams *et al.*, *IEEE Photon. J.*, **6**(5), p. 5501208, 2014.
4. J. Yao, *J. Lightw. Technol.* **27**(3), 314-335, 2009.
5. W. Nget *et al.*, *J. Lightw. Technol.* **9**(9), 1124-1131, 1991.
6. V. Kamanet *et al.*, *IEEE Photon. Technol. Lett.*, **15**(6), pp. 849-851, 2003.
7. J.-D. Shin *et al.*, *IEEE Photon. Technol. Lett.*, **15**(5), pp. 1364-1366, 2004.
8. S. Yegnanarayanan *et al.*, *IEEE Photon. Technol. Lett.*, **9**(5), pp. 634-635, 1997.
9. J. Xie *et al.*, *Opt. Express*, **22**(19), pp. 22707-22715, 2014.
10. P. J. Bocket *et al.*, *Opt. Express*, **18**(19), pp. 20251-20262, 2010.
11. J. Wang *et al.*, *Opt. Express*, **22**(13), pp. 15335-15345, 2014.
12. V. Donzella *et al.*, *Opt. Express*, **22**(17), pp. 21037-21050, 2014.